Metformin Confers Cardiac and Renal Protection in Sudden Cardiac Arrest via AMPK Activation

Cody A. Rutledge[1], Claudia Lagranha[1], Takuto Chiba[2,3], Kevin Redding[1], Donna B. Stolz[4], Sunder Sims-Lucas[2,3], Cameron Dezfulian[5], Jonathan Elmer[6], Brett A. Kaufman[1]

1. Division of Cardiology, Vascular Medicine Institute, Department of Medicine, University of Pittsburgh, Pittsburgh, PA, USA

2. Rangos Research Center, Children's Hospital of Pittsburgh, University of Pittsburgh, Pittsburgh, PA, USA

3. Division of Nephrology, Department of Pediatrics, University of Pittsburgh School, Pittsburgh, PA, USA

4. Department of Cell Biology, University of Pittsburgh, Pittsburgh, PA, USA

5. Department of Critical Care, Texas Children's Hospital, Houston, TX, USA

6. Departments of Emergency Medicine, Critical Care Medicine, and Neurology, University of Pittsburgh, Pittsburgh, PA, USA

Corresponding Author:

Brett A. Kaufman

200 Lothrop Street

BST E1241

Pittsburgh, PA 15261

1-412-624-8644

bkauf@pitt.edu

Conflicts of Interest:

The authors have declared that no conflict of interests exists

Abstract

Sudden cardiac arrest (SCA) affects over 600,000 individuals annually in the United States and is associated with substantial mortality. After resuscitation, multi-system organ damage is common and largely attributable to ischemia-reperfusion injury. The anti-diabetic drug metformin improves cardiac outcomes in models of myocardial ischemia and ischemia-reperfusion. In this study, we evaluated the role of metformin pretreatment in a mouse model of SCA. We found that two weeks of metformin pretreatment protects cardiac ejection fraction and reduces acute kidney injury post-SCA in non-diabetic mice. Further, metformin pretreatment prior to SCA activates AMPK signaling and is associated with altered mitochondrial dynamics and markers of autophagy following arrest. Direct AMPK activation and inhibition studies demonstrate that activation is necessary and sufficient for metformin-mediated protection of cardiac and renal tissues in this model. We were unable to demonstrate cardiac improvement with a single-dose metformin rescue therapy. Importantly, the protective findings translate into patients. We retrospectively evaluated the extent of cardiac and kidney damage in diabetic patients resuscitated from SCA. Metformin-treated patients have less evidence of heart and kidney damage after arrest than diabetics who have not received metformin. Together, these data support AMPK activation as a preventive mechanism in ischemia-reperfusion injury.

43 **Graphical Abstract**

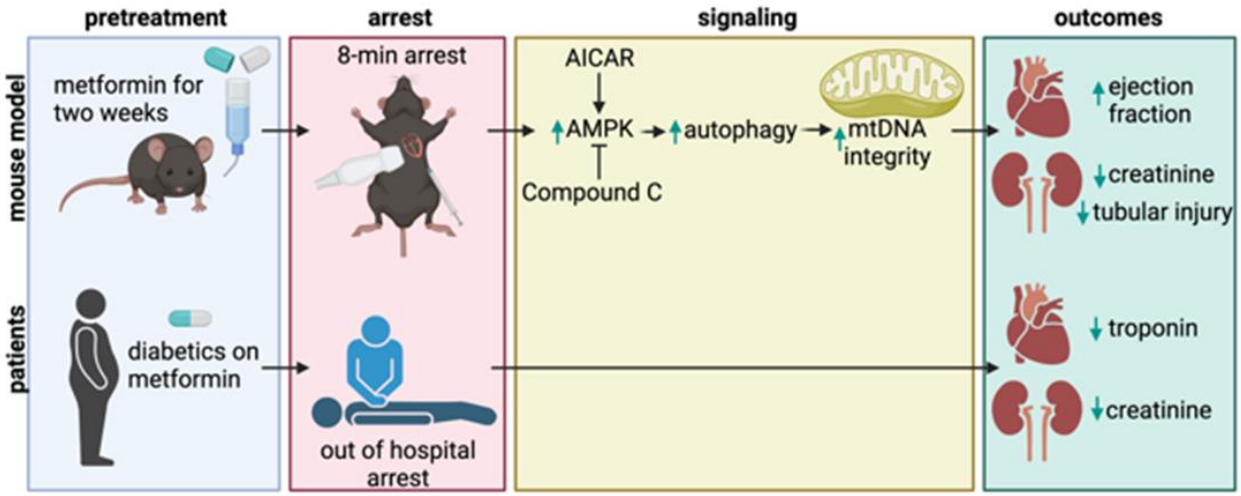

44

45 **Introduction**

46 Sudden cardiac arrest (SCA) refers to the abrupt cessation of cardiac function and affects over
47 600,000 patients annually in the United States (1,2). Patients with return of spontaneous circulation
48 after SCA experience systemic ischemia-reperfusion injury, typically resulting in multi-system organ
49 damage. Common findings include cardiogenic shock, acute renal failure, liver damage, and neurologic
50 dysfunction (3–5). Previous observational studies in cardiac arrest patients have shown that low cardiac
51 ejection fraction (EF) (6) and reduced kidney function (7,8) are predictors of increased mortality. Despite
52 its prevalence, no pharmacologic therapy has been shown to improve overall survival after cardiac
53 arrest.

54 Metformin is an oral antihyperglycemic agent used as the first-line agent for type 2 diabetes
55 that has proven beneficial in a number of cardiovascular conditions (9,10). Metformin enhances insulin
56 sensitivity and normalizes glucose and lipid homeostasis (11–13). Beyond its role in controlling diabetes,
57 metformin has demonstrated clinical benefit across a wide variety of pathologies, including improved
58 mortality in the setting of coronary artery disease (10), congestive heart failure (14), acute kidney injury
59 (AKI)(15), chronic kidney disease (14), septic shock (16,17), and major surgical procedures (18).
60 Cardiovascular studies suggest that improved outcomes occur independently of the glucose-lowering
61 effects of metformin and may instead be attributable to metformin's other pleiotropic effects (19).
62 Several mechanisms beneficial to cardiovascular health have been implicated in metformin's numerous
63 effects, including reduced oxidative stress, anti-apoptotic activities, JNK inhibition, complex I inhibition,
64 and AMPK activation (20,21).

65 Importantly, AMPK activity and expression is induced in mice and humans by ischemic stress as
66 a compensatory response (22). AMPK activity limits endoplasmic reticulum (ER) stress (23) and AMPK
67 deficiency can be partially rescued through reduction of mitochondrial oxidative stress (24). While AMPK
68 activity is essential for survival after ischemic stress (23), it is unclear whether AMPK activity is the
69 mediator of metformin-mediated protection in ischemic heart disease. Furthermore, it is not clear
70 whether the adaptive upregulation of AMPK during cardiac stress is optimal, or whether further
71 activation could even more strongly impact recovery in cardiac injury models.

72 In this study, we sought to test metformin's potential benefit on heart and kidney protection
73 after SCA, both to clarify its relevance to the development of cardiac and peripheral tissue dysfunction,
74 and to determine the role of AMPK in post-arrest outcomes. Therefore, we evaluated outcomes
75 following SCA in mice with chemical activation of AMPK, via 5-aminoimidazole-4-carboxamide-1-β-D-
76 ribofuranoside (AICAR; an AMP-mimetic (25)) and with metformin treatment, and with inhibition of
77 AMPK via compound C (a reversible competitive inhibitor (26)) given concomitantly with metformin
78 treatment. We found that both metformin and AICAR pretreatment improved cardiac and renal
79 outcomes after resuscitation from SCA, and that metformin therapy is associated with altered markers
80 of autophagy and mitochondrial dynamics. We also showed that metformin's benefits are negated by
81 compound C, supporting an AMPK-dependent mechanism. Further, we performed a retrospective
82 analysis of clinical outcomes in diabetic cardiac arrest patients with and without metformin therapy
83 prior to arrest. We found that diabetic patients taking metformin prior to SCA had lower serum markers
84 of cardiac and renal damage 24 hours after arrest than non-metformin diabetic patients. Taken
85 together, we have identified AMPK activity as a protective mechanism invoked SCA-induced damage and

86 demonstrated benefit of metformin pretreatment on cardiac and renal outcomes in SCA, which provides
87 substantial support for metformin's use as a prophylactic in patients at risk for SCA.

88

Results

SCA mice have increased AMPK signaling by pathway analysis

To gain insight into gene expression pathways affected in the heart *in vivo* after SCA, we performed microarray analysis of left ventricles (LVs) 24 hours post-resuscitation. In these initial discovery experiments, male and female mice were evenly divided into untreated sham and untreated arrest groups, where the arrest group underwent ultrasound-guided direct LV injection of potassium chloride (KCl) to cause SCA (Figure 1A). In brief, these mice sustained eight minutes of asystole followed by up to three minutes of cardiopulmonary resuscitation (CPR) until return of spontaneous circulation (ROSC) occurred (Figure 1B). One day after surgery, LV tissue was collected for RNA expression analysis. From Ingenuity Pathway Analysis, *AMPK Signaling* pathway was the most prominent by ranked p-value, while *Autophagy* was the sixth most significantly changed pathway between sham and untreated SCA mice (Figure 1C, Supplemental Figure 1).

Metformin pretreatment protects cardiac EF and kidney function after SCA

AMPK signaling has been shown to be upregulated in myocardial ischemia/reperfusion injury as a compensatory response (27), while the loss of key AMPK subunits increases infarct size in experimental systems (23,24). In *ex vivo* rat hearts, infarct size can be reduced by acute, transitory AMPK activation (28,29). Furthermore, AMPK activation has been shown to delay the progression of heart failure in a chronic pressure overload model (30). Although the etiology of cardiac dysfunction in myocardial infarction and pressure overload is distinct from SCA, we reasoned that further enhancing AMPK activity could provide functional cardiac benefits in the *in vivo* SCA model.

To test this hypothesis, male and female mice were divided into sham and arrest groups, with and without pretreatment of metformin, an established AMPK activator (31). Metformin-treated mice were given 1 mg/mL of metformin in water for two weeks. There were no significant differences among baseline animal characteristics, including ratio of female mice or EF (Table 1, Figure 2A, Supplemental Figure 2). Importantly, there were no differences among groups for body weight in these non-diabetic mice. Twenty-four hours after surgery, untreated arrest mice had significantly lower EF than untreated sham mice (sham: 59.5±1.7%; untreated arrest: 41.1±2.7%, $p<0.0001$, Figure 2A), as expected based on our previous description of this model (32). Importantly, metformin pretreatment significantly improved EF 24 hours post-SCA (arrest metformin: 51.6±2.6%, $p<0.01$ vs. untreated arrest) to a level not significantly different from sham mice (Figure 2A). There were no changes to post-operative body temperature, time to resuscitation, or 24-hour random glucose levels between arrest groups (Table 1). The lack of detectable changes in body weight or in the 24-hour post-SCA glucose suggests that differences in systematic glucose handling was inadequate to explain later phenotypes.

The effects of whole-body ischemia/reperfusion injury can be detected in peripheral tissues, particularly in the kidney (32). Unsurprisingly, untreated arrest mice had significant kidney damage when compared to untreated sham mice at one day post-SCA. Kidney damage was quantified by serum creatinine (sham: 0.36±0.04 mg/dL; untreated arrest: 1.49±0.14 mg/dL, $p<0.0001$, Figure 2B-C) and blood urea nitrogen (BUN) levels (sham: 26.6±5.2 mg/dL; untreated arrest: 153.9±28.4 mg/dL, $p<0.001$), and tubular injury score by histological analysis (sham: 0.11±0.04; untreated arrest: 3.33±0.24, $p<0.0001$). The 1 mg/mL metformin-pretreated arrest mice had some improvement over untreated arrest mice, with reduced creatinine levels (arrest metformin: 0.92±0.24 mg/dL, $p<0.05$ vs. untreated

130 arrest). However, metformin treatment did not fully protect kidneys from SCA-induced damage because
131 serum creatinine was elevated compared to untreated sham ($p<0.05$ vs. sham), as was BUN (121.2±28.0
132 mg/dL, $p<0.05$ vs. sham). Similarly, histological analysis revealed an increase in tubular injury score in
133 arrest metformin mice (2.26±0.24, $p<0.0001$ vs. sham) that was partially improved compared to
134 untreated arrest ($p<0.01$; Figure 2B-C). Metformin pretreatment in sham mice did not significantly affect
135 creatinine levels (0.38±0.06 mg/dL), BUN (28.8±9.4 mg/dL), or tubular injury score (0.14±0.04; Figure 1C)
136 relative to untreated sham. The time of renal ischemia was unchanged between untreated and
137 metformin-pretreated arrest groups (Figure 2D; Table 1), suggesting that reperfusion differences were
138 not a component of metformin-mediated kidney protection.

139 Metformin dosage has been a concern for patients with preexisting kidney damage, especially
140 for those with chronic kidney disease, but lower doses have been found safe and avoid hyperlactatemia
141 (33,34). Furthermore, data have suggested that differences in dosage alter metformin targets, with low
142 doses activating AMPK, but higher doses causing mitochondrial Complex I inhibition (35). We therefore
143 treated an additional mouse cohort with a lower dose of metformin (0.2 mg/mL in drinking water as
144 opposed to 1 mg/mL in Figure 2) to reduce potential complications of decreased metformin clearance
145 after arrest (Supplemental Figure 3A). We found that the low-dose metformin cohort did not have
146 significant cardio-protection when compared to untreated arrest mice (EF of low-dose metformin:
147 50.7±3.3%, n=9, $p=0.08$ vs. untreated arrest, n=20), though this cohort may not have been powered to
148 detect small cardiac changes. However, the low-dose metformin arrest cohort did have lower serum
149 creatinine (0.40±0.05 mg/dL, $p<0.001$ vs. untreated arrest) and BUN levels (64.83±8.24 mg/dL, $p<0.05$
150 vs. untreated arrest), but unchanged tubular injury when compared to untreated arrest mice (2.04±0.71,
151 $p=0.08$ vs. untreated arrest) (Supplemental Figure 3B). These results suggest superior kidney protection
152 with low-dose metformin over the higher dose metformin pretreatment, and protection against
153 ischemia/reperfusion injury by metformin need not be through mitochondrial respiration dysfunction.

154 **Metformin promotes AMPK activation in the LV following SCA**

155 As a marker of total AMPK activation, we assessed phosphorylation of threonine-172 of the
156 AMPKα subunit in the pretreatment cohort (36). One day after surgery, LVs from sham and arrest
157 groups with and without metformin pretreatment (n=6/group) were assessed for p-AMPK, total AMPK,
158 and glyceraldehyde 3-phosphate dehydrogenase (GAPDH) protein expression (Figure 2E). Surprisingly,
159 metformin treatment did not appear to cause activation of p-AMPK/AMPK in the sham mice (untreated
160 sham: 1.00±0.13; metformin sham: 0.80±0.11). However, we found significantly elevated p-AMPK/AMPK
161 in arrest metformin mice (1.52±0.14) when compared to untreated sham (1.00±0.13, $p<0.05$), untreated
162 arrest (0.70±0.12, $p<0.001$), and metformin-pretreated sham mice (0.80±0.11, $p<0.01$). p-AMPK/GAPDH
163 was similarly elevated in the LVs of metformin arrest mice (1.47±0.08) when compared to untreated
164 sham (1.00±0.10, $p<0.05$), untreated arrest (0.90±0.14, $p<0.01$), and metformin-pretreated sham
165 (0.98±0.09, $p<0.05$). Total AMPK/GAPDH was not significantly changed between groups. These data
166 suggest that in this cardiac injury model, metformin pretreatment increases the potential for AMPK
167 activation.

168 **AMPK activation causes cardiac and renal protection after SCA and is necessary for metformin's**
169 **protection of EF**

170 Because metformin has multiple potential modes of action (37), we tested whether direct AMPK
171 activation was necessary and sufficient for the observed enhanced EF, and whether metformin benefit
172 in SCA depended on AMPK activity. To that end, male and female mice were divided into two groups: 1)
173 AICAR pretreatment, which activates AMPK (38), and 2) metformin-pretreatment combined with
174 compound C, an established AMPK inhibitor (13). Both groups underwent two weeks of intraperitoneal
175 (IP) injections prior to SCA and subsequent evaluation 24-hours after arrest. These groups were
176 compared to the untreated arrest and metformin pretreated arrest mouse results described above. One
177 day after surgery, AICAR pretreated arrest mice had significantly improved EF when compared untreated
178 arrest mice (AICAR arrest: 52.0±2.4%, $p<0.05$ vs. untreated arrest, Figure 3A). Compound C not only
179 prevented the beneficial effects of metformin on post-SCA EF, but also caused significantly reduced EF
180 (metformin + compound C arrest: 30.0±2.9%) when compared to untreated arrest ($p<0.05$). There was
181 no change to body weight, ratio of female mice, or baseline EF (Table 1 and Supplemental Figure 2) prior
182 to arrest. The effects of AICAR pretreatment phenocopies metformin pretreatment, and compound C
183 blocks the benefit of metformin strongly suggest that AMPK activation is necessary and sufficient for the
184 metformin-mediated protection of cardiac function after SCA. We cannot rule out the involvement of
185 involvement of glucose homeostasis and insulin sensitivity as contributing factors in this process. We
186 have not observed differences in random glucose and insulin levels, suggesting that such an effect would
187 be modest.

188 To confirm the impact of these compounds on AMPK activity in our model, twenty-four hours
189 after surgery, LVs from arrest groups (n=6) were assessed for AMPK and p-AMPK expression
190 (Supplemental Figure 4). As expected, p-AMPK/AMPK was significantly elevated in AICAR-pretreated
191 arrest mice (AICAR arrest: 2.54±0.59) when compared to untreated arrest (1.00±0.17, $p<0.05$). p-
192 AMPK/GAPDH and AMPK/GAPDH were not significantly changed in the AICAR group. Metformin +
193 compound C pretreated mice had lower p-AMPK/AMPK than the AICAR group (arrest metformin +
194 compound C: 0.52±0.13, $p<0.05$) and p-AMPK/GAPDH (0.54±0.11, $p<0.05$) but no significant change
195 from the untreated arrest group.

196 In the same cohort of mice, measures of kidney damage were significantly lower in AICAR-
197 pretreated mice than untreated arrest mice. Both creatinine (AICAR arrest: 0.67±0.25 mg/dL, $p<0.05$,
198 Supplemental Figure 5A) and tubular injury score (AICAR arrest: 1.45±0.42, $p<0.01$) were significantly
199 improved relative to untreated arrest mice (creatinine 1.49±0.14 mg/dL, tubular injury score 3.33±0.24).
200 In contrast, there was no significant change when comparing renal outcomes in metformin-treated and
201 metformin + compound C-treated arrest mice (Supplemental Figure 5A). AICAR phenocopied the
202 metformin benefit in measures of kidney function and damage, suggesting a role for AMPK activation in
203 those processes. The limited change in these measures in the metformin + compound C cohort vs.
204 untreated arrest mice may suggest that at baseline AMPK activation is limited and cannot be further
205 reduced but would require further experimentation.

206 **Metformin does not improve outcomes as a rescue therapy**

207 In *ex vivo* studies of ischemia-reperfusion, acute metformin administration just prior to stop-
208 flow mediated injury improved developed pressures during recovery (39). In ligation-mediated
209 ischemia/reperfusion experiments *in vivo*, 125 µg/kg metformin injection into the LV lumen at the time
210 of reperfusion resulted in a decreased infarct area and improved EF in non-diabetic mice (40). In
211 contrast to coronary artery ligation experiments, which generally rely on >30 minute ischemic times and

212 generate significant cardiomyocyte death, our SCA model is 8 minutes of ischemia and lacks overt cell
213 death (32). In our SCA model, when metformin was given directly into the LV at resuscitation as a rescue
214 therapy (1,250 µg/kg), there was no change to EF at one day after SCA (arrest rescue metformin:
215 42.1±2.4%) compared to untreated arrest mice (Figure 3B). Similarly, there was no change in creatinine
216 (arrest rescue metformin: 1.2±0.25), BUN (arrest rescue metformin: 155.3±14.2), or tubular injury score
217 (arrest rescue metformin: 2.45±0.55) when compared to untreated arrest mice (Supplemental Figure
218 5B). Baseline EF was not significantly different between groups (Supplemental Figure 2). These data are
219 consistent with the notion that metabolic adaptation is required for the metformin protection after SCA.

220 **Metformin affects mitochondrial morphology and markers of mitochondrial dynamics and autophagy**

221 Because ischemia/reperfusion is well known to induce mitochondrial damage, electron
222 microscopy was used to identify mitochondrial structural changes among in hearts of untreated sham,
223 untreated arrest, and metformin-pretreated arrest mice (Figure 4A). The untreated arrest mice showed
224 a decrease in mitochondrial perimeter and area (perimeter: 3.06±0.06 µm; area: 0.60±0.02 μm^2) when
225 compared to sham (perimeter: 3.81±0.09 µm; area: 0.87±0.04 μm^2, $p<0.0001$ for both measures) in
226 cardiomyocytes (Figure 4B). Myocardium from metformin-pretreated arrest mice showed a modest but
227 significant increase of mitochondrial perimeter and area (perimeter: 3.33±0.07 µm; area: 0.70±0.03
228 μm^2) when compared to that of untreated arrest mice ($p<0.05$ for both measures). Both the untreated
229 arrest mice (0.76±0.001 µm, $p<0.0001$) and metformin-pretreated arrest mouse heart (0.75±0.01 µm;
230 $p<0.0001$) had more circular mitochondria than the untreated sham mouse (0.69±0.01 µm). These data
231 demonstrate changes in mitochondrial morphology at 24 hours post-SCA, with improvements in
232 mitochondrial area and perimeter in metformin-pretreated arrest mice compared to untreated arrest
233 mice.

234 Because of the change in mitochondrial architecture, we also looked at markers of
235 mitochondrial biogenesis and damage in the LVs. First, representative proteins of mitochondrial
236 respiratory complexes were assessed from LV extracts taken 24 hours after arrest from untreated sham,
237 untreated arrest, metformin-pretreated sham, and metformin-pretreated arrest mice (Figure 4C). There
238 was a mild but significant elevation in a subunit of complex II in the metformin-pretreated arrest mice
239 (1.29±0.10) compared to untreated sham mice (0.98±0.04, $p<0.01$); but otherwise, relative expression of
240 representative proteins was unchanged across the groups. Second, we examined mtDNA relative
241 abundance and damage in the cardiac tissue from these groups (Figure 4D). Unlike in failed hearts (41),
242 the arrest group did not show a statistically significant decrease in mtDNA levels at 24 hours post-SCA.
243 The metformin-pretreated arrest mice had slightly higher relative mitochondrial DNA (mtDNA) levels
244 (1.16±0.06) than untreated arrest mice (0.89±0.05, $p<0.05$), but were not significantly different from the
245 sham group (1.00±0.05). Importantly, the metformin-pretreated arrest mice had significantly less
246 mtDNA damage (0.03±0.1 lesions/10kb mtDNA) than untreated arrest mice (0.59±0.16 lesions, $p<0.05$)
247 as measured by long extension PCR assays. The small but significant increases in mtDNA and complex II
248 in the metformin-pretreated arrest mice are consistent with an increase in mitochondrial biogenesis,
249 but the significant improvement in mitochondrial morphology and mtDNA integrity suggests an
250 improvement in overall mitochondrial quality.

251 To understand the alterations in mitochondrial morphology better, we examined the relative
252 levels of several proteins involved in establishing mitochondrial shape (Figure 5A). Mitofusin 2 (MFN2), a
253 mitochondrial outer membrane GTPase involved in fusion, had reduced expression in metformin-

254 pretreated arrest mice (arrest metformin: 0.53±0.07) compared to all other groups (sham: 1.00±0.10,
255 p<0.01; arrest: 1.06±0.07 AU, p<0.001; sham metformin: 0.89±0.04, p<0.05). OPA1, also a dynamin-
256 related GTPase that resides in the inner membrane to perform fusogenic functions (42), followed a
257 similar overall trend with significantly reduced levels in metformin-pretreated arrest mice (0.75±0.04)
258 when compared to untreated arrest mice (1.13±0.10, p<0.05). In contrast, dynamin-related protein 1
259 (DRP1), whose activity is regulated by its phosphorylation at Ser-616 (43), showed no significant change
260 in p-DRP1/DRP1 between sham and arrest groups. Metformin pretreatment appeared to modestly
261 improve p-DRP1/DRP1 post-arrest but the effect was not statistically significant likely because the
262 decline in p-DRP in untreated arrest hearts was not significant. Indeed, while mitochondrial perimeter
263 and area are increasing with metformin-pretreatment in 24 hour post-SCA hearts, markers of fusion
264 decrease and fission are not significantly changed from sham or arrest. The MFN2 decrease may instead
265 suggest that other mitochondrial quality control processes contribute to the improved mitochondrial
266 morphology.

267 Interestingly, the MFN2 decrease is consistent with the activation of autophagy (44,45), where it
268 is ubiquitinated and targeted for proteolysis. Metformin has been reported to impact heart autophagy
269 through AMPK signaling (46,47). To test engagement of autophagy in the SCA model, LVs collected 24
270 hours after SCA from untreated sham, untreated arrest, metformin-pretreated sham, and metformin-
271 pretreated arrest mice were evaluated for markers of autophagy by western blot analysis (Figure 5B).
272 First, we evaluated the mTOR signaling pathway, a crucial negative regulator of autophagy (48).
273 Consistent with prior findings (49), we found the marker of mTOR activity, p-mTOR (Ser-2448), to be
274 significantly reduced in untreated arrest (0.58±0.08, p<0.05), metformin-pretreated sham (0.55±0.08,
275 p<0.05), and metformin-pretreated arrest mice (0.53±0.07, p<0.05) when compared to sham mice
276 (1.0±0.15). Total mTOR protein (mTOR/GAPDH) was only reduced in the metformin-pretreated arrest
277 group (0.71±0.08) when compared to sham (1.00±0.05, p<0.05) and untreated arrest (0.96±0.06,
278 p<0.05) groups. The total activity of mTOR is captured in the p-mTOR per cell (normalized to GAPDH),
279 and the relative activation state of mTOR (p-mTOR/mTOR) is similar. As positive downstream markers of
280 mTOR activity, S6 ribosomal protein (S6) phosphorylation at Ser-240/244 (p-S6) was assessed. As with p-
281 mTOR, both the p-S6/GAPDH and p-S6/S6 were in agreement that the mTOR pathway highest in the
282 untreated sham hearts, with arrest decreasing the mTOR activity. However, because mTOR activity
283 (based on both p-mTOR and p-S6 measures) are not significantly different between arrest and arrest
284 metformin mice, the data suggest that decreased mTOR activation alone is insufficient to explain the
285 survival benefit of metformin.

286 Because metformin has been reported to increase cardiac mitophagy in cardiomyopathy
287 (46,47), we evaluated protein expression for markers associated with autophagosome formation,
288 including p62/Sequestosome 1, a cargo receptor associated with degradation of ubiquinated proteins
289 (50), and LC3 processing (Figure 5B). p62 expression (normalized to GAPDH) was significantly lower in
290 the metformin arrest mice (0.67±0.09) when compared to the untreated arrest group (1.22±0.10,
291 p<0.05, Figure 5B). The relative levels of microtubule-associated protein light chain 3 (LC3), specifically
292 levels of uncleaved (LC3-I) and cleaved (LC3-II) forms, were also monitored as an indicator of changes in
293 autophagy initiation(51). Interestingly, the LC3-II to LC3-I ratio was significantly increased in untreated
294 arrest mice (1.91±0.15) compared to sham (1.00±0.18, p<0.01), whereas the metformin-pretreated
295 arrest mice had significantly reduced LC3-II/LC3-I (1.17±0.17) when compared to untreated arrest mice
296 (p<0.05, Figure 5B). LC3-I and LC3-II expression levels (normalized to GAPDH) were not significantly

297 changed between groups (Supplemental Figure 6). The reduction of p62 and LC3-II/I to untreated sham
298 levels in metformin-pretreated LVs after SCA appears to associate with the improvements in the
299 mitochondrial area and perimeter in the metformin arrest hearts versus the untreated arrest hearts.

300 **Metformin improves markers of cardiac and renal damage in humans one day after SCA**

301 Data supporting metformin use in cardiovascular disease are conflicting, often varying with the
302 particular condition or disease (21). To mirror our observations in mice, we focused this retrospective
303 study on diabetic patients who survived to hospital care after resuscitation from SCA; many of these
304 patients were taking metformin prior to SCA. We started with clinical data from 2,692 patients treated
305 at a single academic medical center, of whom 692 (26%) had a history of diabetes (Figure 6). We
306 excluded 268 patients with chronic kidney disease, 20 who were transferred to the facility more than 24
307 hours post-arrest, 56 for whom home medications were unknown, 7 who rearrested prior to labs being
308 drawn, and 1 who was resuscitated with extracorporeal membrane oxygenation, leaving 341 patients in
309 our final analysis. The mean age was 65 ± 13 years and 148 (43%) were female (Table 2). Overall, 140
310 (41%) patients were prescribed metformin prior to arrest, 153 (45%) were prescribed insulin, and 92
311 (27%) were prescribed other oral hyperglycemic medications. Serum troponin and creatinine were
312 measured as part of routine clinical care, typically at least once daily, which we used to quantify heart
313 and kidney injury, respectively. We did not find reliable echocardiography data in this cohort. Median
314 peak troponin in the first 24 hours post-arrest was 1.4 (interquartile range, IQR: 1.0-1.7) and median
315 peak creatinine was 1.4 (IQR: 1.0-2.0). We used generalized linear models (gamma distribution, log link)
316 to test the independent association of pre-arrest metformin use with peak troponin and creatinine
317 within 24 hours after SCA, adjusting for clinically relevant confounders including age, sex, arrest location
318 (in- vs out-of-hospital), witnessed collapse, layperson CPR, number of epinephrine doses administered,
319 cardiac etiology of arrest, Charlson comorbidity index, and the use of insulin or other oral hyperglycemic
320 medications (Table 2). We handled the 2% missing data using multiple imputations. Metformin
321 prescription at the time of SCA was independently associated with lower 24-hour peak serum troponin
322 and lower 24-hour peak serum creatinine (Table 3). Without A1C levels, we cannot rule out whether
323 there are differences in glycemic control that associate with the improved cardiac and renal measures in
324 these patients.

325 **Discussion**

326 SCA is a common cardiac event for which there are extremely poor outcomes and no current
327 course-altering interventions. Metformin therapy, a first-line diabetes treatment, is beneficial in a
328 number of cardiovascular disorders (9,10), making it a candidate approach for SCA. Metformin impacts
329 many metabolic processes, including activation of the AMPK signaling pathway, improvement in
330 autophagy and mitochondrial biogenesis, and inhibition of the mitochondrial permeability transport
331 pore (mPTP) to block apoptosis (52–56). Metformin, applied as a therapy, decreases scar size in both
332 reversible coronary artery ligation (21,28,40,56–58) and *ex vivo* whole-heart ischemia-reperfusion
333 (21,59). Studies of metformin's effects on cardiac function have largely utilized ischemia-reperfusion
334 injury models like these, with ischemic periods of 25-30 minutes. The long ischemic duration in these
335 models involves substantial cardiomyocyte necrosis, and much of metformin's beneficial effect has been
336 attributed to reduction of mPTP-mediated cell death in the infarct border zone (52). Previous studies
337 have also shown that metformin protects cardiac function acutely through a vasodilatory effect in a rat
338 heart model of cardiac stunning from *ex vivo* ischemia (39). In contrast, our data demonstrate
339 metformin's protection of *in vivo* EF in a SCA model (Figure 2) that features an 8-minute ischemia period
340 without evidence of cardiac cell death (32) (Figure 1). Therefore, using metformin pretreatment and
341 short ischemia, we were able to identify intracellular processes that adapt the cardiomyocyte to
342 maintain function rather than alter cell survival.

343 Metformin pretreatment has pleiotropic effects in which a large number of molecular pathways
344 are implicated, including reducing oxidative stress, inhibiting apoptosis, inhibiting complex I, and
345 activating AMPK signaling (19,21,35,60). Pathway analysis of microarray data from hearts of SCA mice
346 compared to sham mice implicated AMPK signaling as the most significantly changed pathway in our
347 ischemia-reperfusion injury model (Figure 1C). The preservation of cardiac function by metformin and
348 AICAR suggests that additional AMPK activation over that induced by ischemia is both possible and
349 beneficial. Reciprocally, mice that were concomitantly treated with metformin and the AMPK inhibitor
350 compound C had significantly lower EF than untreated arrest mice (Figure 3A). Taken together, these
351 data rigorously support that AMPK activation is sufficient and necessary for cardiac protection.

352 The mechanisms underlying metformin's benefits in our SCA model are difficult to fully
353 elucidate. However, our data indicate that mitochondrial dynamics, including mitochondrial
354 morphology, biogenesis, and turnover, may be central to this benefit. We observed that the
355 mitochondria in LVs of SCA mice are smaller and rounder than sham cohorts, and that metformin-
356 pretreated arrest mice have significantly larger mitochondria then untreated arrest mice (Figure 4),
357 which suggest a possible role for alterations in either mitochondrial dynamics or mitophagy as
358 regulators of mitochondrial morphology. Electron transport chain complex abundance estimates were
359 largely unchanged between treatment groups, except for a mild elevation in complex II expression in the
360 metformin-pretreated arrest mice over the sham cohort (Figure 4B). mtDNA copy number and damage
361 were not significantly elevated in the untreated arrest mice when compared to sham, but metformin
362 pretreatment did drive a small increase in mtDNA copy number (Figure 4D). Importantly, a large
363 decrease mtDNA damage was observed in arrest metformin hearts compared to untreated arrest hearts
364 and untreated sham, focusing attention on a change in mitochondrial turnover.

365 There were notable changes to markers of autophagy and mitochondrial dynamics, both of
366 which have been implicated as pathways altered by AMPK signaling (61–64). We found evidence of

367 decreased expression levels of p-mTOR and p-S6 in untreated arrest, metformin sham, and metformin
368 arrest groups when compared to sham mice (Figure 5B). The decreased mTOR activity could indicate
369 that cells are more poised for autophagy in sham metformin hearts, untreated arrest and metformin-
370 pretreated arrest samples. Importantly, an increase in LC3-II/LC3-I occurred in arrest samples but was
371 completely restored to baseline in metformin-pretreated arrest samples. P62, another classical receptor
372 of autophagy, was not significantly changed in the untreated arrest versus sham samples but was
373 reduced in metformin-pretreated arrest mice compared to untreated arrest (Figure 5B). These findings
374 are consistent with an increase in autophagy with arrest, which was improved by either decreased
375 mitochondrial damage or restored autophagic clearance in the metformin arrest hearts. The data
376 further suggest heightened clearance of damaged mitochondria because mtDNA damage decreased in
377 metformin-pretreated arrest hearts beyond control levels. This concept of cardiac cells being poised for
378 autophagy is consistent with our observation from metformin rescue therapy, which would not allow
379 adaptation for improved autophagy and failed to improve EF after SCA (Figure 3B).

380 Based on morphology, SCA causes an increase in mitochondrial fission relative to untreated
381 sham in the heart (Figure 5). Metformin pretreatment improves mitochondrial morphology but does not
382 significantly modulate the fission regulator DRP1. Furthermore, it is unlikely that metformin
383 pretreatment increases fusion, as fusogenic proteins MFN2 and OPA1 are both further depleted in
384 metformin arrest mice relative to the arrest mice. Importantly, depletion of MFN2 and OPA1 is
385 associated with the induction of autophagy (65), suggesting that mitochondrial clearance is enhanced in
386 the metformin-treated SCA mice. Although this study lacks directed measures of mitochondrial flux, the
387 data are consistent with the explanation that metformin pretreatment decreased proteotoxic stress in
388 hearts and caused more efficient turnover of mitochondria (e.g. (46)) and removal of damaged mtDNA,
389 therefore increasing the overall quality of the mitochondria and cardiac function at 24 hours post-arrest.

390 Metformin pretreatment also protects against kidney injury in our model of SCA, reducing
391 creatinine levels, BUN, and tubular injury scores (Figure 2). As there is no change to ischemic duration in
392 the kidneys between untreated arrest and metformin-pretreated arrest mice, as measured by renal
393 artery doppler ultrasound (Table 1), this renal protection is potentially intrinsic to the kidney rather than
394 secondary to the improved cardiac function. Previous studies have demonstrated beneficial effects of
395 metformin on renal performance after primary renal ischemic injury (66–68). Our model extends the
396 known impact of metformin on renal function by demonstrating comparable beneficial effects in a
397 model featuring renal ischemia secondary to cardiac arrest, more analogous to clinically observed renal
398 injury.

399 There exists concern about metformin therapy in the presence of kidney injury, as metformin
400 accumulation can lead to potentially lethal lactic acidosis (34). While we did not assess lactate build-up
401 or metformin accumulation in our model, we did treat an additional cohort of mice with a lower dose of
402 metformin (Supplemental Figure 3), comparable to concentrations of human doses, to address concerns
403 about supra-pharmacologic metformin concentrations (69). We found that low-dose metformin
404 conferred better renal protection than standard-dose metformin, as measured by creatinine levels after
405 arrest (Supplemental Figure 3B). However, cardiac EF improvement did not reach significance in the low-
406 dose group. There has been some concern about the mechanism of action in high-dose vs. low-dose
407 metformin therapy; recent work has demonstrated that supra-pharmacologic doses of metformin effect
408 change through inhibition of mitochondrial ATP production, whereas pharmacological doses of
409 metformin increase mitochondrial respiration and fission (70). The literature would suggest that our

410 high-dose metformin (1 mg/mL) is a Complex I inhibitor(71), whereas low-dose metformin (0.2 mg/mL)
411 activates AMPK and triggers mitochondrial fission(70). Our work did not confirm or explore the
412 mechanistic differences between these two doses, but in the context of SCA, metformin is not inducing
413 fission at the high dose, nor is Complex I inhibition in the heart the likely cause because both low and
414 high doses are cardio- and renal protective.

415 To evaluate the clinical relevance of the cardiac and renal protection demonstrated with
416 metformin pretreatment in our SCA mouse model, we performed a retrospective analysis of diabetic
417 patients resuscitated from cardiac arrest. We divided these patients into metformin-treated and non-
418 metformin-treated patients. Generalized linear models demonstrated a significant association between
419 metformin pretreatment and decreased peak serum troponin and peak serum creatinine levels within
420 24 hours post-arrest (Table 3). This suggests that metformin is driving cardiac and renal protection,
421 respectively, independently of other baseline characteristics. Previous studies have noted that improved
422 renal function after arrest is predictive of long-term outcomes (7,8). It is not clear, however, whether or
423 not early cardiac outcomes are predictive of survival (6,72). Our analysis was not powered to look for
424 survival benefit in human subjects, but such a study is warranted.

425 In summary, we provide evidence in both a mouse model and retrospective clinical study that
426 metformin pretreatment offers significant cardiac and renal protection acutely after SCA. Our SCA
427 mouse involves cardiac injury without cardiac cell death, making it a more focused system in which to
428 study metformin's mechanism of action. Direct AMPK activation and inhibition studies confirmed that
429 AMPK activation is necessary and sufficient for the cardiac and renal benefits observed with metformin
430 treatment. A number of molecular mechanisms exist downstream of AMPK activation, and we have
431 implicated changes to autophagy and mitochondrial dynamics in our mouse studies, though there were
432 no dramatic changes to mitochondrial morphology or electron transport chain subunit expression.
433 Future studies are warranted to investigate which signaling and metabolic pathways regulate improved
434 clearance of damaged mitochondria. Results may inform potential acute rescue therapies for ischemia-
435 reperfusion injury that replicate the cardiac and renal protection seen in our mouse model and patient
436 studies. In addition, larger studies of SCA populations may provide additional clinical parameters
437 important for metformin-mediated improvements in cardiac and renal function and ultimately recovery.

438

439

440 **Methods**

441 **Pre-clinical Data**

442 **Sudden Cardiac Arrest Model**

443 Eight-week-old male and female C57BL/6J mice (Jackson Labs, Bar Harbor, ME, #000664)
444 underwent cardiac arrest by delivery of potassium chloride (KCl) directly into the LV by percutaneous,
445 ultrasound-guided needle injection as previously described (32). Briefly, mice were anesthetized using
446 vaporized isoflurane (Henry Schein, Melville, NY, #1182097) and endotracheally intubated, then
447 mechanically ventilated (MiniVent, Harvard Apparatus, Holliston, MA, #73-0043) at a rate of 150 bpm
448 and volume of 125 µL for females and 140 µL for males. Body temperature was maintained by utilizing a
449 rectal temperature probe and heating pad (Indus Instruments, Webster, TX, #THM150). The chest was
450 cleaned of hair using Nair and sterilized with betadine prior to introduction of a 30-gauge needle into
451 the LV under ultrasound guidance (Visual Sonics Vevo 3100 with Vevo LAB v 5.5.1 software, Toronto,
452 Canada), followed by delivery of 40 µL of 0.5M KCl to induce asystole. The ventilator was discontinued,
453 and mice remained in asystole for a total of 8 minutes. 7.5 minutes after KCl dosing, 500 µL of 15 µg/mL
454 epinephrine in saline (37°C) was injected into the LV over approximately 30 seconds. At 8 minutes, CPR
455 was initiated by finger compression at about 300 bpm for 1-minute intervals. Electrocardiogram (ECG)
456 was evaluated for return of sinus rhythm after each 1-minute interval. Animals not achieving ROSC by 3
457 minutes after CPR initiation were euthanized. Mice remained on the ventilator until breathing frequency
458 was greater than 60 times per minute. Sham mice received no KCl, but rather a single injection of
459 epinephrine. All animals were placed in a recovery cage under a heat lamp after the procedure.

460 **Animal Treatment Groups**

461 Treatment groups in the study were as follows: untreated sham, untreated cardiac arrest,
462 metformin-pretreated sham, metformin-pretreated cardiac arrest, 5-aminoimidazole-4-carboxamide-1-
463 beta-D-ribofuranoside (AICAR) pretreated cardiac arrest, metformin + compound c pretreated cardiac
464 arrest, metformin rescue treatment cardiac arrest, and low-dose metformin pretreatment cardiac
465 arrest. Metformin pretreatment consisted of *ad libitum* access to metformin (Major Pharmaceuticals,
466 Livonia, MI, #48152) in drinking water (1 mg/mL) for 14 days prior to surgery. AICAR pretreated mice
467 were given IP injections of 500 mg/kg AICAR (Toronto Research Chemicals, Toronto, CA, #A611700) in
468 saline every other day for 14 days prior to surgery. Compound C pretreated mice were given 20 mg/kg IP
469 injections of compound C (Cayman Chemical, Ann Arbor, MI, #11967) in saline daily for 14 days prior to
470 arrest. Metformin rescue therapy was given as a single direct LV injection (1250 µg/kg) dissolved in
471 saline along with 500 µL of 1mg/mL epinephrine (Par Pharmaceutical, Chestnut Ridge, NY, #10977) at
472 the time of resuscitation. Low-dose metformin pretreatment consisted of *ad libitum* access to
473 metformin in drinking water (0.2 mg/mL) for 14 days prior to surgery.

474 **Echocardiography and Ultrasound**

475 Immediately prior to arrest surgery, mice were evaluated by transthoracic echocardiography
476 using Vevo 3100 imaging systems (Visual Sonics) with a 40MHz probe. Repeat echocardiography was
477 performed one day after arrest under isoflurane anesthesia delivered by nose cone. Heart rate was
478 maintained between 400-500 bpm during imaging by adjusting isoflurane concentration. B-mode images
479 taken from the parasternal long-axis were captured and LV EF calculated using modified Simpson's

480 methods (73). A cohort of all groups were assessed for renal perfusion after resuscitation. The
481 ultrasound probe was oriented transversely across the abdomen at the plane of the right kidney and
482 monitored for renal artery blood flow by doppler imaging. Image analysis was performed by a blinded
483 sonographer (Vevo Lab 5.5.1, Visual Sonics).

484 **Tissue and Serum Collection**

485 After euthanasia with isoflurane and cervical dislocation, mice underwent cardiac puncture for
486 collection of blood by heparinized syringe. Blood was separated by centrifugation at 2,000 x g at 4°C for
487 10 minutes and the serum was flash frozen. These samples were evaluated for blood urea nitrogen
488 (BUN), creatinine, alanine aminotransferase (ALT), and creatine kinase (CK) by the Kansas State
489 Veterinary Diagnostic Laboratories (Manhattan, KS). Hearts from the mice were excised and LVs were
490 isolated and flash frozen.

491 **Western Blot**

492 Frozen LV tissue was homogenized in lysis buffer containing a protease/phosphatase cocktail
493 (Sigma-Aldrich, St. Louis, MO, #11697498001) and normalized for protein content using a BCA assay (Life
494 Technologies, Carlsbad, CA, #23235). Samples were separated on NuPage 4-12% gradient SDS-PAGE gels
495 (ThermoFisher, Waltham, MA, #WG1403BOX) and transferred onto iBlot nitrocellulose membranes
496 (Invitrogen, #IB301001). Membranes were blocked in 5% milk for 1 hour and then incubated overnight
497 at 4°C with primary antibodies, including OxPhos Rodent Antibody Cocktail 1:5000 (ThermoFisher,
498 #458099), p-AMPK (Thr172, 1:1000, Cell Signaling, Danvers, MA, #2535), AMPK (1:1000, Cell Signaling,
499 #2532), p-mTOR (Ser2448, 1:1000, Cell Signaling, #2971), DRP1 (1:1000, Cell Signaling, #5391), pDRP1
500 (Ser616, 1:1000, Thermo, #PA5-64821), mTOR (1:1000, Cell Signaling, #2972), p-S6 (Ser240/244, 1:1000,
501 Cell Signaling, #2215), S6 (1:1000, Cell Signaling, #2217), p-AKT (Ser473, 1:1000, Cell Signaling, #9271),
502 AKT (1:1000, Cell Signaling, #9272), p62 (1:1000, Sigma-Aldrich, #P0067), and GAPDH (1:5000, Millipore,
503 St. Louis, MO, #AB2302). Following incubation, membranes were washed with TBS-tween and then
504 probed for 1 hour at room temperature with anti-mouse or anti-rabbit secondary antibodies (Jackson
505 ImmunoResearch, West Grove, PA, #115-035-003 and #115-035-144). Images were obtained by
506 developing on a ChemiDoc XRS imaging system (BioRad, Hercules, CA) and analyzed using ImageJ
507 software (National Institutes of Health, Bethesda, MD).

508 **Tissue Histology**

509 Kidneys were fixed overnight in 10% formalin (Thermo, #SF100) at 4°C, then washed with PBS
510 and transferred to 70% ethanol at room temperature. After fixation and dehydration, tissues were
511 embedded in paraffin prior to sectioning at 4 µm by the Histology Core at the Children's Hospital of
512 Pittsburgh. Sections were stained with hematoxylin and eosin (H&E). Renal tubular pathology was semi-
513 quantitatively scored (0: no injury to 4: severe injury) in terms of tubular dilatation, formation of
514 proteinaceous casts, and loss of brush border(74). Histological scoring was performed in a blinded
515 fashion at 40x magnification on outer medullary regions of the tissue sections. Eight fields were
516 evaluated per kidney (n=6-8 animals/group). Samples were imaged using a Leica DM 2500 microscope
517 (Leica, Wetzlar, Germany) and analyzed with LAS X software (Leica).

518 **Transmission Electron Microscopy**

519 LV tissue was immersion fixed in 2.5% glutaraldehyde in 0.1M PBS overnight at 4°C. Fixed
520 samples were washed 3x in PBS then post-fixed in aqueous 1% OsO_4, 1% $K_3Fe(CN)_6$ for 1 hour at room

521 temperature. Following 3 PBS washes, the pellet was dehydrated through a graded series of 30-100%
522 ethanol, and then 100% propylene oxide then infiltrated in 1:1 mixture of propylene oxide:Polybed 812
523 epoxy resin (Polysciences, Warrington, PA) for 1 hour. After several changes of 100% resin over 24
524 hours, the samples were embedded in molds and cured at 37°C overnight, followed by additional
525 hardening at 65°C for two more days. Semi-thin (300 nm) sections were heated onto glass slides, stained
526 with 1% toluidine blue and imaged using light microscopy to assure proper tissue orientation. Ultrathin
527 (60-70 nm) sections were collected on 100 mesh copper grids, and stained with 4% uranyl acetate for 10
528 minutes, followed by 1% lead citrate for 7 min. Sections were imaged using a JEOL JEM 1400 PLUS
529 transmission electron microscope (Peabody, MA) at 80 kV fitted with a side mount AMT digital camera
530 (Advanced Microscopy Techniques, Danvers, MA). Twenty random images were obtained from sections
531 throughout each LV. Individual mitochondria (n=50/sample) were randomly selected and traced for
532 blinded quantification of size, roundness, and density via ImageJ (v1.8.0) software (75).

533 **RNA Isolation, qPCR, and Microarray Analysis**

534 Total genomic and mitochondrial DNA were isolated from frozen, powdered LV tissue. Tissue
535 was homogenized in a buffer containing Proteinase K digestion buffer and proteinase K (Genesee
536 Scientific, Genesee, NY, #42-700) overnight at 55°C, as previously described (76,77). The next day, DNA
537 was purified by centrifuging the homogenized buffer with staged EtOH resuspension, followed by
538 centrifugation and resuspension in TE buffer supplemented with RNase A (Invitrogen, #12091039). DNA
539 concentration was measured using an AccuBlue Broad Range kit (Biotium, Fremont, CA, #31009).
540 Relative mtDNA abundance was measured using a TaqMan primer/probe for mitochondrial ND1 (VIC-
541 labeled; primer:probe 1:1) versus nuclear HDAC1 (FAM-labeled; primer:probe of 3:1; Supplemental
542 Table 1). Multiplex assessment of relative abundance of mtDNA was quantified using real-time
543 quantitative PCR (qPCR) with TaqMan Fast Advanced Master Mix (ThermoFisher, #4444965) performed
544 on QuantStudio 5 PCR system (Applied Biosystems). 4.6 ng of DNA was included in each reaction with 5
545 µM of primers/probes in a 10 µL total reaction volume and calculated by the ΔΔCq method (78). The
546 qPCR amplification profile was: one cycle (95°C for 20 seconds) followed by 40 cycles (95°C for 1 sec
547 then 60°C for 20 seconds). All primers and probes were produced by Integrated DNA Technologies
548 (Coralville, Iowa).
549
550 mtDNA damage was assessed by comparing total PCR product after long-amplicon mtDNA
551 replication with LongAmp Hot Start Taq Polymerase (New England Biolabs, Ipswich PA, #M0533;
552 Supplemental Table 1) (79). 15 ng of DNA was amplified using the following profile: one cycle (94°C for 2
553 minutes) followed by 17 cycles (94°C for 15 seconds then 64°C for 12 seconds) then 1 cycle (72°C for 10
554 min)(80). Final product was measured by Accublue within the linear detection range. Specific DNA
555 products were confirmed by gel electrophoresis.
556
557 Microarray analysis was performed on cDNA through the Affymetrix microarray analysis service
558 (ThermoFisher). Eight untreated sham and eight untreated arrest mice were included in these studies
559 with an even distribution of males and females. Differential gene expression analysis was performed
560 using Transcription Analysis Console (Thermofisher). Gene-level p-values less than 0.05 were considered
561 significant for gene inclusion. Subsequent pathway analysis was performed to compare untreated sham
562 and arrest groups through Ingenuity Pathway Analysis (Qiagen). Complete datasets were deposited in
563 GEO (accession no. GSE176494).
564
565 **Statistical Analysis**
566

567 Data were expressed as mean ± standard error in all figures. $p \leq 0.05$ was considered significant
568 for all comparisons. One-way ANOVA with either Dunnett's multiple comparisons test or Tukey's
569 multiple comparisons post-hoc analysis was used to compare groups either to a single group or all
570 groups as detailed in figure legends. All statistical analysis was completed using Graphpad Prism 8
571 software (San Diego, CA).

572 **Clinical Data**
573
574 **Clinical Data Collection**
575
576 De-identified adult patients with a documented history of diabetes mellitus treated at a single
577 academic medical center after resuscitation from cardiac arrest from January 2010 to December 2019
578 were included in this study. Patients with a history of known kidney disease prior to arrest, patients who
579 arrived at our facility over 24 hours after collapse, patients for whom home medications were unknown,
580 patients who rearrested and died before blood work could be acquired, and patients resuscitated with
581 extracorporeal support were excluded from analysis. Demographic and arrest characteristics from a
582 prospective registry, including patient age, sex, shockable presenting arrest rhythm, witnessed arrest,
583 layperson CPR, arrest duration, number of epinephrine doses administered, cardiac etiology of arrest,
584 and Charlson Comorbidity Index were extracted. Admission pharmacy documentation in each patient's
585 electronic medical record was evaluated to determine whether patients were prescribed metformin,
586 insulin, or other oral antihyperglycemic medications prior to their arrest, and classified each of these as
587 three independent binary predictors. The primary outcomes of interest were peak serum creatinine and
588 peak serum troponin at 24 hours post-arrest.

589 **Clinical Statistical Analysis**

590 Baseline population characteristics and outcomes were summarized using descriptive statistics.
591 Multiple imputation with chained equations with predictive mean matching was used to impute missing
592 continuous variables. Generalized linear models with a gamma distribution and log link were used to
593 test the association of metformin with peak 24-hour serum creatinine and peak 24-hour serum
594 troponin. For primary adjusted analysis, covariates were included based on biological plausibility. A
595 series of sensitivity analyses, including a backward stepwise model sequentially removing predictors
596 with $p<0.1$, complete case analysis, and adjusted modeling were performed, excluding patients receiving
597 insulin who may be fundamentally sicker than those receiving no medications or oral antihyperglycemics
598 only.

599 **Study Approvals**

600 All mouse studies were performed at the University of Pittsburgh in compliance with the
601 National Institutes of Health Guidance for Care and Use of Experimental Animals. This protocol was
602 approved by the University of Pittsburgh Animal Care and Use Committee (Protocol #18032212). The
603 University of Pittsburgh Human Research Protection Office approved all aspects of the reported human
604 subject's research with a waiver of informed consent due to its no greater than minimal risk to
605 participants (STUDY19020205).

Author Contributions

CR, CD, and BK were responsible for conceptualization of these studies. CR designed the methodology and with CL and KR performed the investigation. CR and JE were responsible for data curation. Formal analyses were performed by CR, CL, TC, SSL, CD, and JE. Visualization was completed by TC and DS. CR, SSL, CD, JE, and BK wrote the manuscript. SSL and BK supervised the project, and BK provided resources for its completion. All authors reviewed the final manuscript and are responsible for its integrity.

Acknowledgements

Research reported in this manuscript was supported by: American Heart Association Transformational Project Award 18TPA34230048, NIH Instrument Grant for Advanced High-Resolution Rodent Ultrasound Imaging System 1S10OD023684-01A1, NIH Training Program in Imaging Sciences in Translational Cardiovascular Research 5T32HL129964-02, NIH 5K23NS097629 (to JE), and Richard K. Mellon Institute Award for postdoctoral trainees (to TC). Graphical abstract created with BioRender.com.

621 **References**

622 1. Aparicio HJ, Benjamin EJ, Callaway CW, et al. *Heart Disease and Stroke Statistics-2021 Update A*
623 *Report from the American Heart Association*.; 2021. doi:10.1161/CIR.0000000000000950

624 2. Zipes D, Wellens HJJ. Sudden Cardiac Death. *Circulation*. 1998;98(21):2334-2351.

625 3. Mongardon N, Dumas F, Ricome S, et al. Postcardiac arrest syndrome: from immediate
626 resuscitation to long-term outcome. *Ann Intensive Care*. 2011;1(45):1-11.

627 4. Neumar RW, Nolan JP, Adrie C, et al. Post-cardiac arrest syndrome: Epidemiology,
628 pathophysiology, treatment, and prognostication a consensus statement from the International
629 Liaison Committee on Resuscitation. *Circulation*. 2008;118(23):2452-2483.
630 doi:10.1161/CIRCULATIONAHA.108.190652

631 5. Ruiz-Bailén M, Aguayo De Hoyos E, Ruiz-Navarro S, et al. Reversible myocardial dysfunction after
632 cardiopulmonary resuscitation. *Resuscitation*. 2005;66(2):175-181.
633 doi:10.1016/j.resuscitation.2005.01.012

634 6. Chang WT, Ma MHM, Chien KL, et al. Postresuscitation myocardial dysfunction: Correlated
635 factors and prognostic implications. *Intensive Care Med*. 2007;33(1):88-95. doi:10.1007/s00134-
636 006-0442-9

637 7. Park YS, Choi YH, Oh JH, et al. Recovery from acute kidney injury as a potent predictor of survival
638 and good neurological outcome at discharge after out-of-hospital cardiac arrest. *Crit Care*.
639 2019;23(1):1-11. doi:10.1186/s13054-019-2535-1

640 8. Storm C, Krannich A, Schachtner T, et al. Impact of acute kidney injury on neurological outcome
641 and long-term survival after cardiac arrest – A 10 year observational follow up. *J Crit Care*.
642 2018;47:254-259. doi:10.1016/j.jcrc.2018.07.023

643 9. Maruthur NM, Tseng E, Hutfless S, Wilson LM, Suarez-cuervo C. Diabetes Medications as
644 Monotherapy or Metformin-Based Combination Therapy for Type 2 Diabetes. *Ann Intern Med*.
645 2016;164:740-751. doi:10.7326/M15-2650

646 10. Han Y, Xie H, Liu Y, Gao P, Yang X, Shen Z. Effect of metformin on all-cause and cardiovascular
647 mortality in patients with coronary artery diseases: a systematic review and an updated
648 meta-analysis. *Cardiovasc Diabetol*. 2019;18(96):1-16. doi:10.1186/s12933-019-0900-7

649 11. Stumvoll M, Nurjhan N, Perriello G, Dailey G, Gerich JE. Metabolic Effects of Metformin in Non-
650 Insulin-Dependent Diabetes Mellitus. *N Engl J Med*. 1995;333(9):550-554.
651 doi:10.1056/nejm199508313330903

652 12. Wiernsperger NF, Bailey CJ. The Antihyperglycaemic Effect of Metformin. *Drugs*. 1999;58:31-39.
653 doi:10.2165/00003495-199958001-00009

654 13. Zhou G, Goodyear LJ, Moller DE, et al. Role of AMP-activated protein kinase in mechanism of
655 metformin action Find the latest version : Role of AMP-activated protein kinase in mechanism of
656 metformin action. *J Clin Invest*. 2001;108(8):1167-1174. doi:10.1172/JCI200113505.Introduction

657 14. Crowley MJ, Diamantidis CJ, Mcduffie JR, et al. Clinical Outcomes of Metformin Use in
658 Populations With Chronic Kidney Disease , Congestive Heart Failure, or Chronic Liver Disease. *Ann*
659 *Intern Med*. 2017;166:191-200. doi:10.7326/M16-1901

660 15. Bell S, Farran B, Mcgurnaghan S, et al. Risk of acute kidney injury and survival in patients treated
661 with Metformin: an observational cohort study. *BMC Nephrol*. 2017;18(163):1-8.
662 doi:10.1186/s12882-017-0579-5

663 16. Hassan FI, Sc M, Didari T, et al. A Review on The Protective Effects of Metformin in Sepsis-
664 Induced Organ Failure. 2020;21(4). doi:10.22074/cellj.2020.6286.Introduction

665 17. Jochmans S, Alphonsine JE, Chelly J, et al. Does metformin exposure before ICU stay have any
666 impact on patients' outcome? A retrospective cohort study of diabetic patients. *Ann Intensive*
667 *Care*. 2017;7(116):1-9. doi:10.1186/s13613-017-0336-8

668 18. Reitz K, Marroquin O, Zenati M, et al. Association Between Preoperative Metformin Exposure and
669 Postoperative Outcomes in Adults With Type 2 Diabetes. *JAMA Surg*. 2020;155(6).
670 doi:10.1001/jamasurg.2020.0416.Association

671 19. Cameron AR, Morrison VL, Levin D, et al. Anti-Inflammatory Effects of Metformin Irrespective of
672 Diabetes Status. *Circ Res*. 2016;119:652-665. doi:10.1161/CIRCRESAHA.116.308445

673 20. Chen Q, Lesnefsky EJ. Metformin and myocardial ischemia and reperfusion injury: Moving toward
674 "prime time" human use? *Transl Res*. 2020;229:1-4. doi:10.1016/j.trsl.2020.10.006

675 21. Higgins L, Palee S, Chattipakorn SC, Chattipakorn N. Effects of metformin on the heart with
676 ischaemia-reperfusion injury: Evidence of its benefits from in vitro, in vivo and clinical reports.
677 *Eur J Pharmacol*. 2019;858(April):172489. doi:10.1016/j.ejphar.2019.172489

678 22. Kim TT, Dyck JRB. Is AMPK the savior of the failing heart? *Trends Endocrinol Metab*.
679 2015;26(1):40-48. doi:10.1016/j.tem.2014.11.001

680 23. Cao Y, Bojjireddy N, Kim M, et al. Activation of γ2-AMPK suppresses ribosome biogenesis and
681 protects against myocardial ischemia/reperfusion injury. *Circ Res*. 2017;121(10):1182-1191.
682 doi:10.1161/CIRCRESAHA.117.311159

683 24. Zaha V, Qi D, Su K, et al. AMPK Is Critical for Mitochondrial Function during Reperfusion. *J Mol*
684 *Cell Cardiol*. 2017;21(2):129-139. doi:10.1016/j.yjmcc.2015.12.032.AMPK

685 25. Sullivan J, Brocklehurst K, Marley A, Carey F, Carling D, Beri R. Inhibition of lipolysis and
686 lipogenesis in isolated rat adipocytes with AICAR, a cell-permeable activator of AMP-activated
687 protein kinase. *FEBS Lett*. 1994;353:33-36.

688 26. Liu X, Chhipa RR, Nakano I, Dasgupta B. The AMPK inhibitor compound C is a potent AMPK-
689 independent antiglioma agent. *Mol Cancer Ther*. 2014;13(3):596-605. doi:10.1158/1535-
690 7163.MCT-13-0579

691 27. Dyck JRB, Lopaschuk GD. AMPK alterations in cardiac physiology and pathology: enemy or ally ? *J*
692 *Physiol*. 2006;1:95-112. doi:10.1113/jphysiol.2006.109389

693 28. Paiva MA, Gonçalves LM, Providência LA, Davidson SM, Yellon DM, Mocanu MM. Transitory
694 activation of AMPK at reperfusion protects the ischaemic-reperfused rat myocardium against
695 infarction. *Cardiovasc Drugs Ther*. 2010;24(1):25-32. doi:10.1007/s10557-010-6222-3

696 29. Paiva MA, Rutter-Locher Z, Gonçalves LM, et al. Enhancing AMPK activation during ischemia
697 protects the diabetic heart against reperfusion injury. *Am J Physiol - Hear Circ Physiol*.
698 2011;300(6):2123-2134. doi:10.1152/ajpheart.00707.2010

699 30. Cates C, Rousselle T, Wang J, et al. Activated protein C protects against pressure overload-
700 induced hypertrophy through AMPK signaling. *Biochem Biophys Res Commun*. 2018;495(4):1-18.
701 doi:10.1016/j.bbrc.2017.12.125.Activated

702 31. Rena G, Hardie DG, Pearson ER. The mechanisms of action of metformin. *Diabetologia*.
703 2017;60(9):1577-1585. doi:10.1007/s00125-017-4342-z

704 32. Rutledge CA, Chiba T, Redding K, et al. A novel ultrasound-guided mouse model of sudden cardiac
705 arrest. *PLoS One*. 2020;15(12):1-14. doi:10.1371/journal.pone.0237292

706 33. Lalau JD, Kajbaf F, Bennis Y, Hurtel-Lemaire AS, Belpaire F, De Broe ME. Metformin Treatment in
707 Patients With Type 2 Diabetes and Chronic Kidney Disease Stages 3A, 3B, or 4. *Diabetes Care*.
708 2018;41(3):547-553. doi:10.2337/dc17-2231

709 34. Lalau JD, Arnouts P, Sharif A, De Broe ME. Metformin and other antidiabetic agents in renal
710 failure patients. *Kidney Int*. 2015;87(2):308-322. doi:10.1038/ki.2014.19

711 35. Mohsin AA, Chen Q, Quan N, et al. Mitochondrial complex I inhibition by metformin limits
712 reperfusion injury. *J Pharmacol Exp Ther*. 2019;369(2):282-290. doi:10.1124/jpet.118.254300

713 36. Stein SC, Woods A, Jones NA, Davison MD, Cabling D. The regulation of AMP-activated protein
714 kinase by phosphorylation. *Biochem J*. 2000;345(3):437-443. doi:10.1042/0264-6021:3450437

715 37. Xu X, Lu Z, Fassett J, et al. Metformin protects against systolic overload-induced heart failure
716 independent of AMP-activated protein kinase α2. *Hypertension*. 2014;63(4):723-728.
717 doi:10.1161/HYPERTENSIONAHA.113.02619

718 38. Corton JM, Gillespie JG, Hawley SA, Hardie DG. 5-Aminoimidazole-4-Carboxamide
719 Ribonucleoside: A Specific Method for Activating AMP-Activated Protein Kinase in Intact Cells?
720 *Eur J Biochem*. 1995;229(2):558-565. doi:10.1111/j.1432-1033.1995.tb20498.x

721 39. Legtenberg RJ, Houston RJF, Oeseburg B, Smits P. Metformin improves cardiac functional
722 recovery after ischemia in rats. *Horm Metab Res*. 2002;34(4):182-185. doi:10.1055/s-2002-26705

723 40. Calvert JW, Gundewar S, Jha S, et al. Acute metformin therapy confers cardioprotection against
724 myocardial infarction via AMPK-eNOS- mediated signaling. *Diabetes*. 2008;57(3):696-705.
725 doi:10.2337/db07-1098

726 41. Karamanlidis G, Nascimben L, Couper GS, Shekar PS, Del Monte F, Tian R. Defective DNA
727 replication impairs mitochondrial biogenesis in human failing hearts. *Circ Res*. 2010;106(9):1541-
728 1548. doi:10.1161/CIRCRESAHA.109.212753

729 42. Ge Y, Shi X, Boopathy S, McDonald J, Smith AW, Chao LH. Two forms of Opa1 cooperate to
730 complete fusion of the mitochondrial inner-membrane. *Elife*. 2020;9:1-22. doi:10.1101/739078

731 43. Marsboom G, Toth PT, Ryan JJ, et al. Dynamin-related protein 1-mediated mitochondrial mitotic
732 fission permits hyperproliferation of vascular smooth muscle cells and offers a novel therapeutic
733 target in pulmonary hypertension. *Circ Res*. 2012;110(11):1484-1497.
734 doi:10.1161/CIRCRESAHA.111.263848

735 44. Xiong W, Ma Z, An D, et al. Mitofusin 2 participates in mitophagy and mitochondrial fusion
736 against angiotensin II-induced cardiomyocyte injury. *Front Physiol*. 2019;10(APR):1-12.
737 doi:10.3389/fphys.2019.00411

738 45. Benischke AS, Vasanth S, Miyai T, et al. Activation of mitophagy leads to decline in Mfn2 and loss
739 of mitochondrial mass in Fuchs endothelial corneal dystrophy. *Sci Rep*. 2017;7(1):1-11.
740 doi:10.1038/s41598-017-06523-2

741 46. Kanamori H, Naruse G, Yoshida A, et al. Metformin Enhances Autophagy and Provides
742 Cardioprotection in δ-Sarcoglycan Deficiency-Induced Dilated Cardiomyopathy. *Circ Hear Fail*.
743 2019;12(4):1-13. doi:10.1161/CIRCHEARTFAILURE.118.005418

744 47. Xie Z, Lau K, Eby B, et al. Improvement of cardiac functions by chronic metformin treatment is
745 associated with enhanced cardiac autophagy in diabetic OVE26 mice. *Diabetes*. 2011;60(6):1770-
746 1778. doi:10.2337/db10-0351

747 48. Sciarretta S, Maejima Y, Zablocki D, Sadoshima J. The Role of Autophagy in the Heart. *Annu Rev*
748 *Physiol*. 2018;80:1-26. doi:10.1146/annurev-physiol-021317-121427

749 49. Wu X, He L, Cai Y, et al. Induction of autophagy contributes to the myocardial protection of
750 valsartan against ischemia-reperfusion injury. *Mol Med Rep*. 2013;8(6):1824-1830.
751 doi:10.3892/mmr.2013.1708

752 50. Seibenhener ML, Babu JR, Geetha T, Wong HC, Krishna NR, Wooten MW. Sequestosome 1/p62 Is
753 a Polyubiquitin Chain Binding Protein Involved in Ubiquitin Proteasome Degradation. *Mol Cell*
754 *Biol*. 2004;24(18):8055-8068. doi:10.1128/mcb.24.18.8055-8068.2004

755 51. Li L, Xu J, He L, et al. The role of autophagy in cardiac hypertrophy. *Acta Biochim Biophys Sin*
756 *(Shanghai)*. 2016;48(6):491-500. doi:10.1093/abbs/gmw025

757 52. Emelyanova L, Bai X, Yan Y, et al. Biphasic effect of metformin on human cardiac energetics.
758 *Transl Res*. Published online 2020. doi:10.1016/j.trsl.2020.10.002

759 53. Zhou G, Myers R, Li Y, et al. Role of AMP-activated protein kinase in mechanism of metformin
760 action. *J Clin Invest*. 2001;108(8):1167-1174. doi:10.1172/JCI13505

761 54. Lesnefsky EJ, Chen Q, Hoppel CL. Mitochondrial Metabolism in Aging Heart. *Circ Res*.
762 2016;118(10):1593-1611. doi:10.1161/CIRCRESAHA.116.307505

763 55. Wang X, Yang L, Kang L, et al. Metformin attenuates myocardial Ischemia-reperfusion injury via
764 Up-regulation of antioxidant enzymes. *PLoS One*. 2017;12(8):1-13.
765 doi:10.1371/journal.pone.0182777

766 56. Whittington HJ, Hall AR, McLaughlin CP, Hausenloy DJ, Yellon DM, Mocanu MM. Chronic
767 metformin associated cardioprotection against infarction: Not just a glucose lowering
768 phenomenon. *Cardiovasc Drugs Ther*. 2013;27(1):5-16. doi:10.1007/s10557-012-6425-x

769 57. Solskov L, Løfgren B, Kristiansen SB, et al. Metformin induces cardioprotection against
770 ischaemia/reperfusion injury in the rat heart 24 hours after administration. *Basic Clin Pharmacol*
771 *Toxicol*. 2008;103(1):82-87. doi:10.1111/j.1742-7843.2008.00234.x

772 58. Gundewar S, Calvert, John W, Jha S, et al. Activation of AMPK by Metformin Improves Left
773 Ventricular Function and Survival in Heart Failure. *Circ Res*. 2009;454(1):42-54.
774 doi:10.1161/CIRCRESAHA.108.190918.Activation

775 59. Bhamra GS, Hausenloy DJ, Davidson SM, et al. Metformin protects the ischemic heart by the Akt-
776 mediated inhibition of mitochondrial permeability transition pore opening. *Basic Res Cardiol*.

2008;103(3):274-284. doi:10.1007/s00395-007-0691-y

60. Lesnefsky EJ, Chen Q, Tandler B, Hoppel CL. Mitochondrial Dysfunction and Myocardial Ischemia-Reperfusion: Implications for Novel Therapies. *Annu Rev Pharmacol Toxicol*. 2017;57:535-565. doi:10.1146/annurev-pharmtox-010715-103335

61. Moussa A, Li J. AMPK in myocardial infarction and diabetes: the yin/yang effect. *Acta Pharm Sin B*. 2012;2(4):368-378. doi:10.1016/j.apsb.2012.06.001

62. Takagi H, Matsui Y, Hirotani S, Sakoda H, Asano T, Sadoshima J. AMPK mediates autophagy during myocardial ischemia in vivo. *Autophagy*. 2007;3(4):405-407. doi:10.4161/auto.4281

63. Toyama E, Herzig S, Courchet J, et al. AMP-activated protein kinase mediates mitochondrial fission in response to energy stress. *Sci Rep*. 2016;351(6270):275-282.

64. Wang Q, Wu S, Zhu H, et al. Deletion of PRKAA triggers mitochondrial fission by inhibiting the autophagy-dependent degradation of DNM1L. *Autophagy*. 2017;13(2):404-422. doi:10.1080/15548627.2016.1263776

65. Vásquez-Trincado C, García-Carvajal I, Pennanen C, et al. Mitochondrial dynamics, mitophagy and cardiovascular disease. *J Physiol*. 2016;594(3):509-525. doi:10.1113/JP271301

66. Wang M, Weng X, Guo J, Chen Z, Jiang G, Liu X. Metformin alleviated EMT and fibrosis after renal ischemia-reperfusion injury in rats. *Ren Fail*. 2016;38(4):614-621. doi:10.3109/0886022X.2016.1149770

67. Corremans R, Vervaet BA, D'haese PC, Neven E, Verhulst A. Metformin: A candidate drug for renal diseases. *Int J Mol Sci*. 2019;20(1):1-15. doi:10.3390/ijms20010042

68. Li J, Gui Y, Ren J, et al. Metformin protects against cisplatin-induced tubular cell apoptosis and acute kidney injury via AMPKα-regulated autophagy induction. *Sci Rep*. 2016;6(April):1-11. doi:10.1038/srep23975

69. Cao J, Meng S, Chang E, et al. Low concentrations of metformin suppress glucose production in hepatocytes through AMP-activated protein kinase (AMPK). *J Biol Chem*. 2014;289(30):20435-20446. doi:10.1074/jbc.M114.567271

70. Wang Y, An H, Liu T, et al. Metformin Improves Mitochondrial Respiratory Activity through Activation of AMPK. *Cell Rep*. 2019;29(6):1511-1523.e5. doi:10.1016/j.celrep.2019.09.070

71. Madiraju AK, Erion DM, Rahimi Y, et al. Metformin suppresses gluconeogenesis by inhibiting mitochondrial glycerophosphate dehydrogenase. *Nature*. 2014;510(7506):542-546. doi:10.1038/nature13270.Metformin

72. Jentzer JC, Chonde MD, Dezfulian C. Myocardial Dysfunction and Shock after Cardiac Arrest. *Biomed Res Int*. 2015;2015:1-14.

73. Lang RM, Bierig M, Devereux RB, et al. Recommendations for chamber quantification: A report from the American Society of Echocardiography's guidelines and standards committee and the Chamber Quantification Writing Group, developed in conjunction with the European Association of Echocardiograph. *J Am Soc Echocardiogr*. 2005;18(12):1440-1463. doi:10.1016/j.echo.2005.10.005

74. Chiba T, Peasley KD, Cargill KR, et al. Sirtuin 5 regulates proximal tubule fatty acid oxidation to

816 protect against AKI. *J Am Soc Nephrol*. 2019;30(12):2384-2398. doi:10.1681/ASN.2019020163

817 75. Schneider CA, Rasband WS, Eliceiri KW. NIH Image to ImageJ: 25 years of image analysis. *Nat*
818 *Methods*. 2012;9(7):671-675. doi:10.1038/nmeth.2089

819 76. Kolesar JE, Wang CY, Taguchi Y V, Chou S, Kaufman BA. Two-dimensional intact mitochondrial
820 DNA agarose electrophoresis reveals the structural complexity of the mammalian mitochondrial
821 genome. 2013;41(4):1-14. doi:10.1093/nar/gks1324

822 77. Falabella M, Kolesar JE, Wallace C, et al. G-quadruplex dynamics contribute to regulation of
823 mitochondrial gene expression. *Sci Rep*. 2019;9(5605):1-17. doi:10.1038/s41598-019-41464-y

824 78. Livak KJ, Schmittgen TD. Analysis of relative gene expression data using real-time quantitative
825 PCR and the 2-ΔΔCT method. *Methods*. 2001;25(4):402-408. doi:10.1006/meth.2001.1262

826 79. Gonzalez-Hunt CP, Rooney JP, Ryde IT, Anbalagan C, Joglekar R, Meyer JN. PCR-Based Analysis of
827 Mitochondrial DNA Copy Number, Mitochondrial DNA Damage, and Nuclear DNA Damage. *Curr*
828 *Protoc Toxicol*. 2016;67(1):20.11.1-20.11.25. doi:10.1002/0471140856.tx2011s67

829 80. Furda AM, Bess AS, Meyer JN, Van Houten B. Analysis of DNA damage and repair in nuclear and
830 mitochondrial DNA of animal cells using quantitative PCR. *Methods Mol Biol*. 2012;920:111-132.
831 doi:10.1007/978-1-61779-998-3-9

832

833

834 **Figures and Figure legends**

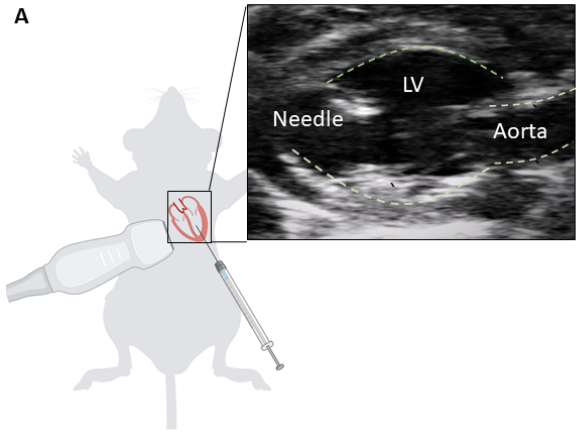

C

IPA Canonical Pathway	-log(p-val)	z-score
AMPK Signaling	5.38	2.121
NRF2-mediated Oxidative Stress	5.05	1.604
Xenobiotic Metabolism PXR Signaling	4.51	2.469
Hepatic Fibrosis	4.5	n/a
HIF1α Signaling	4.48	1.067
Autophagy	4.46	n/a
Insulin Receptor Signaling	3.97	1.3
Apelin Adipocyte Signaling Pathway	3.96	2.837
Unfolded Protein Response	3.9	0
TCA Cycle II (Eukaryotic)	3.76	2.53

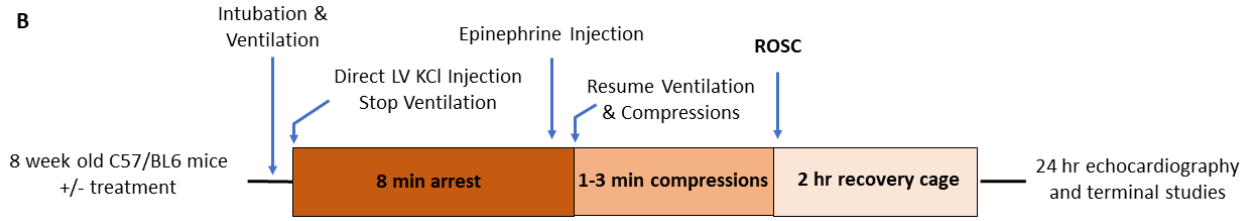

835

836 **Figure 1. Mouse model of sudden cardiac arrest (SCA) and Microarray Pathway Analysis.** A) Cartoon
837 representation of direct left ventricular injection of potassium chloride (KCl) to cause asystole with
838 representative ultrasound image of needle guidance. B) Time course of SCA protocol. C) Pathway
839 analysis of microarray data from left ventricles (LVs) collected one day after SCA (n=8) versus sham (n=8)
840 surgeries, demonstrating the ten most significantly changed canonical signaling pathways by Ingenuity
841 Pathway Analysis (IPA). LV, left ventricle; ROSC, return of spontaneous circulation.

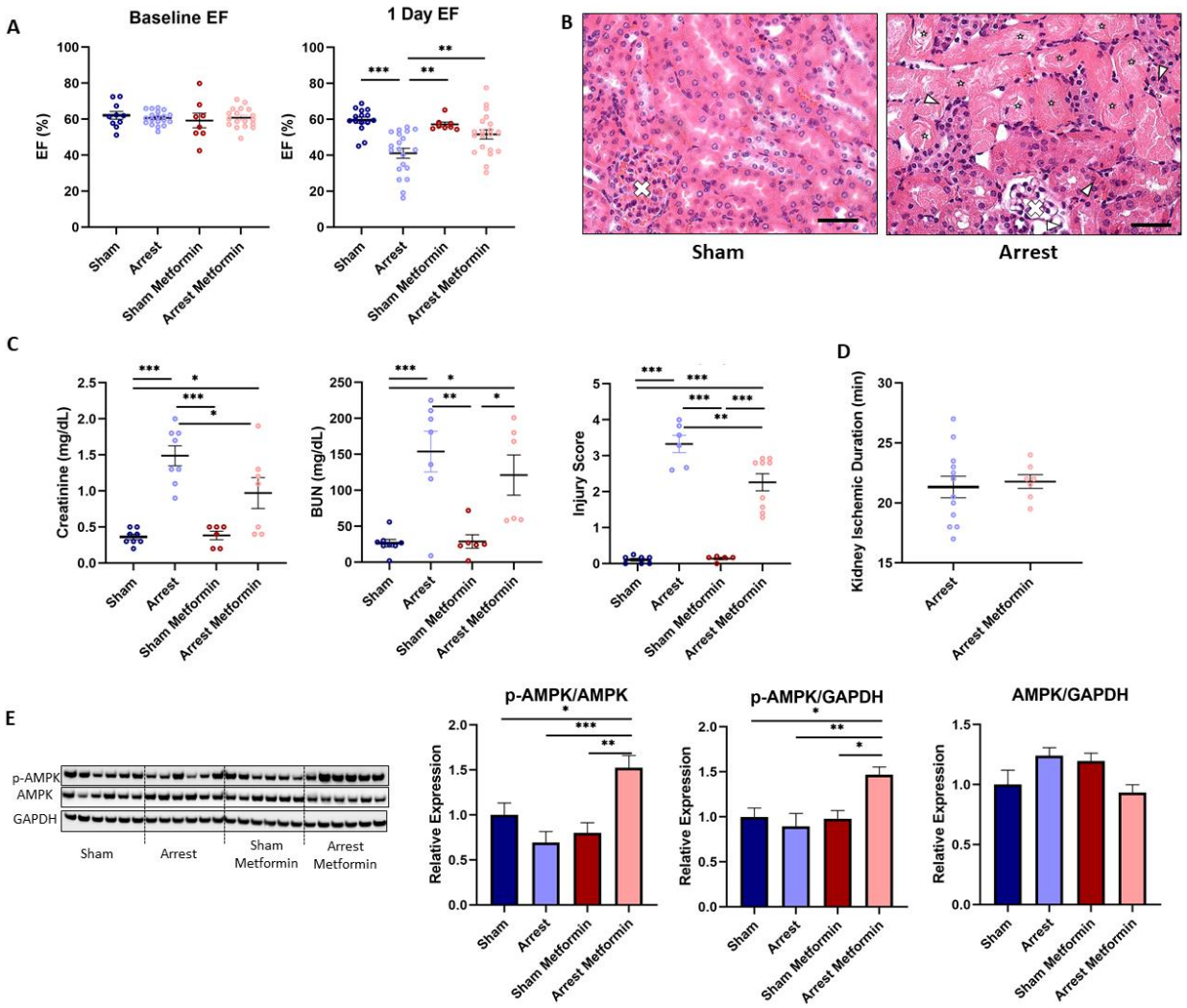

Figure 2. Metformin treated mice have preserved ejection fraction (EF) and lower kidney damage than untreated mice one day after sudden cardiac arrest (SCA). A) Baseline and one day EF among treatment groups. Circles represent individual mice (arrest mice, n=20; sham mice, n=15; sham metformin, n=8; arrest metformin, n=20). B) Representative histologic sections from untreated sham and untreated arrest mice demonstrating proteinaceous casts in renal tubules (black stars) and infiltrates (white arrowheads) with glomeruli marked (white X's). Scale bar = 50 µm. C) Markers of kidney damage, including serum creatinine, blood urea nitrogen (BUN), and histologic tubular injury score. D) Renal ischemic duration in untreated arrest and metformin-treated arrest mice. E) Western blot analysis of pAMPK/AMPK, p-AMPK/GAPDH and AMPK/GAPDH in sham, arrest, sham metformin, and arrest metformin mice (n=6 for all groups). Data are expressed as mean ± SEM. P-values: *< 0.05, **< 0.01, ***< 0.001 by one-way ANOVA with Tukey post-hoc analysis. EF, ejection fraction; BUN, blood urea nitrogen.

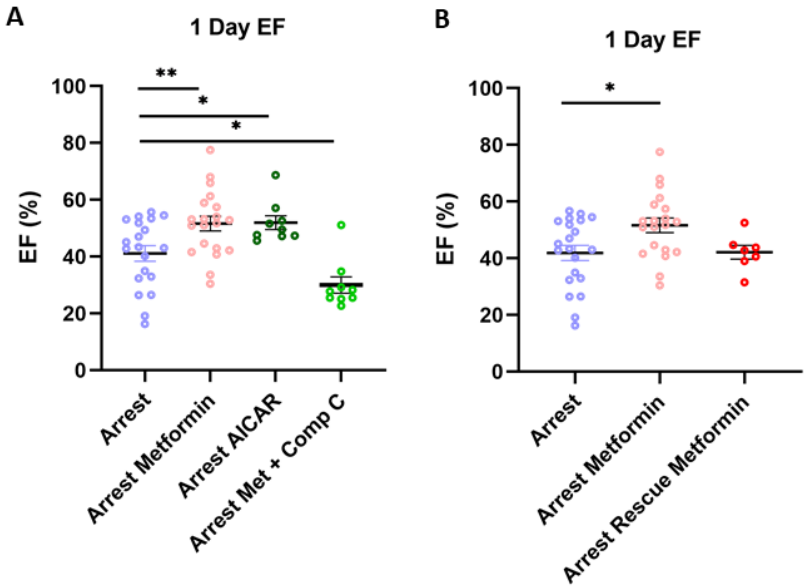

856

857 **Figure 3. AMPK activation alone improves cardiac outcomes after SCA, and AMPK activation is**
858 **necessary to exert metformin's cardioprotection.** A) One-day ejection fraction (EF) in SCA mice
859 pretreated with the AMPK-activator AICAR (Arrest AICAR; n=9) or the AMPK-inhibitor compound C
860 (Arrest Met + Comp C; n=9). Arrest and arrest metformin are shown for comparison (n=15; data
861 presented in Figure 2). B) One-day EF of intravenous metformin administered concomitantly with
862 epinephrine (n=6 for all groups). Data are expressed as mean ± SEM. P-values: *< 0.05, **< 0.01, ***<
863 0.001 by one-way ANOVA with Dunnett's post-hoc analysis (against arrest). AICAR, 5-aminoimidazole-4-
864 carboxamide-1-β-D-ribofuranoside; Comp C, compound C; EF, ejection fraction.

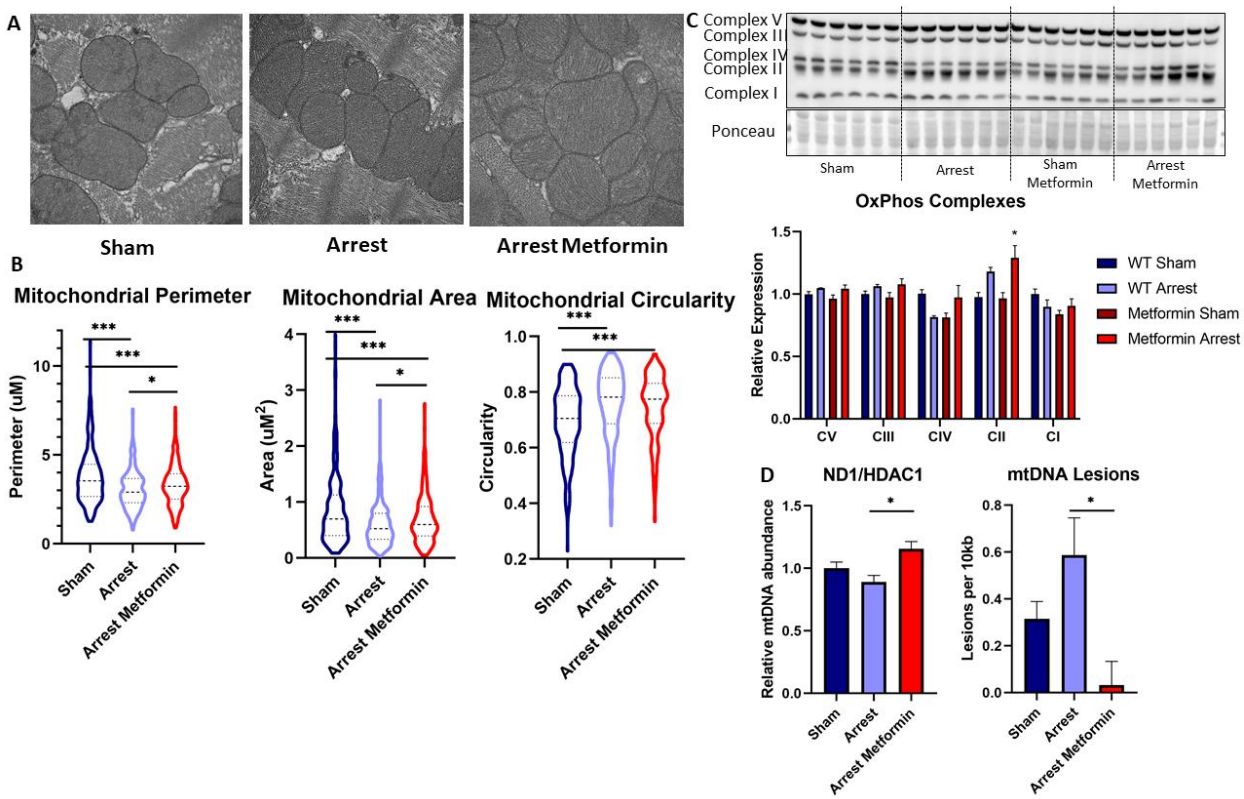

Figure 4. Metformin affects mitochondrial characteristics after SCA. A) Representative electron microscope images of intrafibrillar mitochondria in sham, arrest, and arrest metformin mice one day after surgery (40,000x magnification). B) Violin plot showing mitochondrial perimeter, area, and circularity across sham, arrest, and arrest metformin mice (n=50 per group). C) Western blot of representative oxidative phosphorylation complex subunits (CI-CV) and bar graph of densitometry (n=6/group, normalized to ponceau stain). D) Bar graph of mtDNA copy number assessment by qPCR quantitation of total DNA preparations of sham (n=5), arrest (n=4), and arrest metformin (n=7) mice. Data are expressed as mean ± SEM. P-values: *< 0.05, **< 0.01, ***< 0.001 by one-way ANOVA with Tukey's post-hoc analysis. ND1, NADH dehydrogenase 1; HDAC1, Histone deacetylase 1; mtDNA, mitochondrial DNA; WT, wild-type.

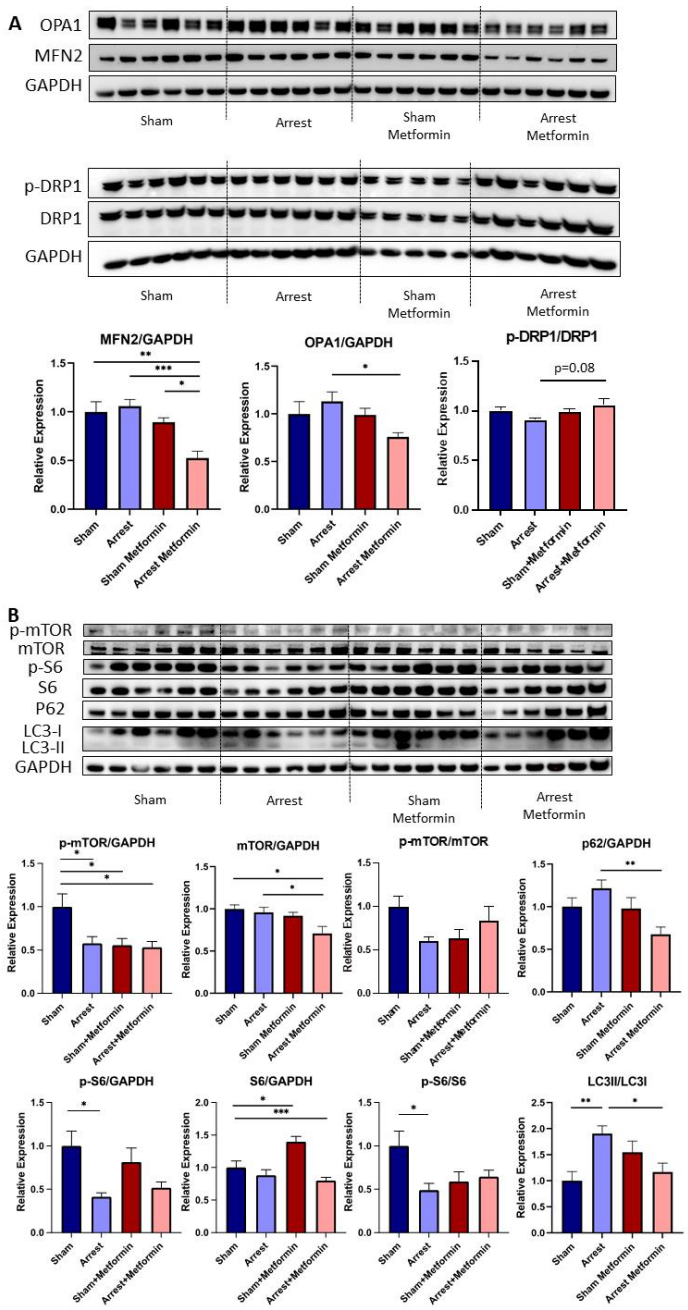

Figure 5. Metformin pretreatment affects expression of mitochondrial fission/fusion proteins and autophagy regulatory genes after sudden cardiac arrest (SCA). A) Representative western blot images of markers of mitochondrial fission and fusion (MFN2, OPA1, p-DRP1, DRP1) and housekeeping protein (GAPDH) in sham (n=6), arrest (n=6), sham metformin (n=5-6), and arrest metformin (n=6) mice. Quantitation shown in bar graphs with indicated normalization. B) Representative western blot images of autophagy-related proteins downstream of AMPK (p-mTOR, mTOR, p62, p-S6, S6, LC3 (I/II)) and housekeeping protein (GAPDH) expression in sham, arrest, sham metformin, and arrest metformin mice (n=6/group). Data are expressed as mean ± SEM. P-values: *< 0.05, **< 0.01, ***< 0.001 by one-way ANOVA with Tukey's post-hoc analysis for all groups. DRP, dynamin-related protein1; LC3, microtubule-associated protein light chain; MFN2, mitofusin 2; mTOR, mechanistic target of rapamycin; OPA1, dynamin-like 120 kDa protein, mitochondrial.

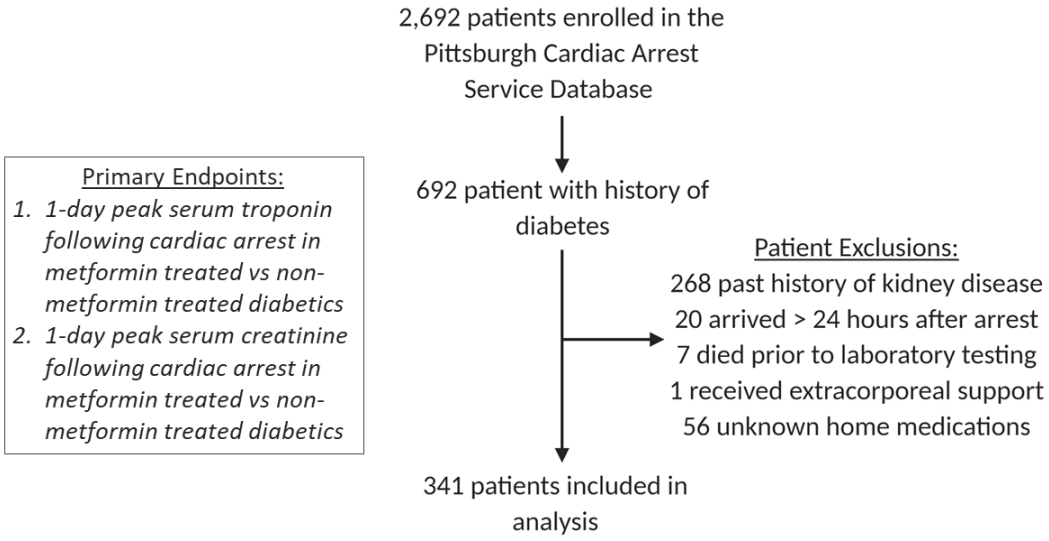

Figure 6. Summary of clinical inclusion and exclusion data for retrospective analysis of the Pittsburgh Post-Cardiac Arrest Service patient database. Primary outcomes evaluated included peak serum troponin and peak serum creatinine in diabetic patients with (n=122) and without (n=174) a history of metformin therapy.

893 **Tables**

894 **Table 1. Surgical data for arrest mice.** There are no significant changes to body weight or body
895 temperature at time of extubation between treatment groups. There is no change in time to return of
896 spontaneous circulation (ROSC) or time to extubation between arrest and arrest metformin groups.
897 There is no change to random blood glucose 24 hours after arrest between sham, arrest, and arrest
898 metformin mice. Data are presented as mean ± SEM unless otherwise noted. Analysis by one-way
899 ANOVA with Tukey's post-hoc analysis.

	Sham (n=20)	**Arrest (n=26)**	**Sham Metformin (n=8)**	**Arrest Metformin (n=21)**	**Arrest Low Dose Metformin (n=9)**	**Arrest AICAR (n=9)**	**Arrest Metformin + Compound C (n=8)**	**Arrest Rescue Metformin (n=7)**
Age (d)	57.55 ± 0.68	57.60 ± 0.59	58.75 ± 0.40	58.80 ± 0.48	60.33 ± 0.53	58.44 ± 0.50	58.75 ± 0.37	60.71 ± 0.61
# Female / Total Mice (percent)	11/20 (55%)	12/26 (46%)	5/8 (63%)	12/21 (57%)	4/9 (44%)	4/9 (44%)	4/8 (50%)	3/7 (43%)
Body Wt (g)	23.19 ± 0.83	22.97 ± 0.62	21.05 ± 0.88	21.77 ± 0.78	20.86 ± 0.84	22.59 ± 1.1	22.47 ± 1.23	22.46 ± 1.34
Temp at Extubation (°C)	35.86 ± 0.15	35.53 ± 0.20	35.96 ± 0.18	35.95 ± 0.12	35.53 ± 0.21	35.79 ± 0.19	36.21 ± 0.11	35.86 ± 0.23
ROSC (min)	-	1.31 ± 0.09	-	1.43 ± 0.15	1.11 ± 0.11	1.44 ± 0.24	1.13 ± 0.12	1.29 ± 0.18
Time to Extubation (min)	-	22.31 ± 0.66	-	23.64 ± 0.32	22.72 ± 0.49	22.06 ± 0.90	24.06 ± 0.52	22.71 ± 0.84
Time to Kidney Reperfusion (min)	-	21.3 ± 0.90	-	21.79 ± 0.57	22.24 ± 0.49	20.43 ± 1.01	24.70 ± 0.64	22.50 ± 0.97
Random glucose 24 h after arrest (mmol/L)	184.3 ± 25.0	205.8 ± 10.0	-	218.8 ± 28.0	-	-	-	-

900

901

902 **Table 2. Baseline demographics and clinical characteristics.** Data are presented as mean ± standard
903 deviation, median [interquartile range], or sample number (corresponding percentage).

Characteristic	Overall cohort (n = 341)	Metformin (n = 140)	No metformin (n = 201)
Age, years	65 ± 13	65 ± 12	64 ± 14
Female sex	148 (43)	58 (41)	90 (45)
Arrest out-of-hospital	256 (75)	108 (77)	148 (74)
Shockable rhythm	109 (32)	39 (28)	70 (35)
Witnessed collapse	160 (47)	70 (50)	90 (45)
Layperson CPR	156 (46)	72 (51)	84 (42)
Epinephrine doses	2 [1 – 4]	3 [1 – 4]	2 [1 – 4]
Arrest duration, min	16 [8 – 27]	16 [8 – 32]	16 [8 – 23]
Cardiac etiology	96 (28)	36 (26)	60 (30)
Charlson Comorbidity index	2 [2 – 3]	2 [1 – 3]	3 [2 – 3]
Insulin	152 (45)	34 (24)	118 (59)
Other oral diabetic medication	92 (27)	47 (34)	45 (22)
Peak 24h troponin	0.88 [0.19 – 5.7]	0.97 [0.29 – 4.71]	0.84 [0.14 – 7.0]
Peak 24h creatinine	1.4 [1.0 – 2.0]	1.3 [1.0 – 1.7]	1.6 [1.0 – 2.1]

904

905

906 **Table 3. Association between metformin use and peak serum creatine and troponin by log link model.**
907 Model was adjusted for age, sex, arrest location (in- vs out-of-hospital), witnessed collapse, layperson
908 cardiopulmonary resuscitation, presenting rhythm, arrest duration, number of epinephrine doses
909 administered, cardiac etiology of arrest, Charlson Comorbidity index, insulin, and other oral diabetic
910 medications. Both peak serum creatinine level and peak serum troponin level 24 hours post-arrest are
911 significantly associated with history of metformin use.

912

Endpoint	**Coefficient (95% CI)**	**P value**
Creatinine	-0.19 (-0.30 – -0.08)	0.001
Troponin	-1.29 (-2.11 – -0.46)	0.002

913

914